CHARACTERIZATION OF IPOMOEA BATATAS 'CILEMBU' NON-TYPICAL AGRICULTURAL LAND USING THE ELECTRICAL RESISTIVITY TOMOGRAPHY (ERT) AND MICROTREMOR APPROACH

Teuku AS[1], Muhammad LA[1] and Edlyn YN[2]

[1]*Geophysical Engineering, Faculty of Mining and Petroleum Engineering, Institute of Technology Bandung, Indonesia*
[2]*Geophysical Engineering, Institute of Technology Sumatera, Indonesia*

Abstract: Soil characterization investigations for the distribution of fertile soils have been carried out on non-typical agricultural lands with the aim that farmers can assess soil fertility problems which can increase crop productivity. This characterization was carried out using a high-precision agricultural approach with currently developing geophysical technology. The geoelectrical method is one of the geophysical methods that can be used to map spatial and temporal variations of soil physical properties. while Microtremor measurements can also be used in soil structure surveys to determine subsurface conditions. From these two methods, data were processed using geopsy software and RES2DINV which produced parameters of dominant frequency (f0), amplification (A), and resistivity (ρ). The processing results obtained resistivity values from 100 to 600 Ωm, dominant frequency values from 3.697 to 4.545 Hz and amplification values from 3.1 to 5.4. The study area shows resistivity values ranging from 100 to 600 Ωm, this indicates an alluvial soil type area that is rich in minerals and suitable for cultivating organic Cilembu sweet potato. This agricultural area also has a frequency value below 4 which indicates that the area has thick sediment, this is due to the decreasing topography of the land from east to west so that there are differences in elevation on agricultural land. This agricultural area also has an amplification value above 4 which indicates that in this area the soil is heterogeneous, dense enough to allow the soil to absorb water better so that in that area the soil is more fertile than soil with low amplification (< 4).

Keywords: Cicalengka, ERT, Microtremor, Agriculture Geophysics, Cilembu sweet potato

Introduction

The market demand for Cilembu sweet potato production is increasing every year. Therefore, this must be balanced with a continuous supply of improved productivity and quality. The challenge in increasing the supply is that Cilembu sweet potatoes with the best yield and quality only grow in the specific Cilembu region. To preserve the Cilembu sweet potato variety and its commercial potential, efforts must be made to find alternative lands suitable for the required conditions and characteristics for cultivating Cilembu sweet potato varieties. Another alternative is to address the issues with atypical Cilembu sweet potato lands. If a solution to this problem can be found, these uncommon soils can help enhance the

Corresponding Author's Email: tasanny.bhtv@gmail.com

yield and quality of Cilembu sweet potato varieties. Therefore, this research is essential to identify the characteristics of atypical soils necessary to address quality and productivity issues on such soils. Consequently, these unusual soils can increase Cilembu sweet potato production to meet market demand.

Soil quality is generally associated with soil fertility for agriculture, determined by the interaction of various physical, chemical, and biological properties within the soil where plant roots are actively engaged. To detect lands with good fertility over a large area, creating a soil classification map that indicates signs of adequate fertility in Cilembu sweet potato lands is necessary. This enables farmers to assess soil fertility issues based on the obesity increase in harvest yields and to factor it into fertilizer recommendations for Cilembu sweet potato lands.

Soil classification mapping can be achieved using high-precision agricultural methods with evolving geophysical technology, such as *Electrical Resistivity Tomography* (ERT). Geoelectrical methods allow for the spatial and temporal mapping of soil physical properties. Unlike traditional soil observations, geoelectrics are non-destructive and provide continuous, large-scale measurements, making them valuable for monitoring variables like soil moisture and nutrient content. Typically, geoelectrical research has focused on determining soil moisture or mineral content in agricultural soils.

Recently, near-surface methods like the *Horizontal-to-Vertical Spectral Ratio* (HVSR) microseismic approach have been used to identify agricultural soils. Microtremors are low-amplitude vibrations in the soil caused by natural or human activities. The Nakamura HVSR method is used to estimate subsurface resonance properties. Microtremor measurements are mainly used in soil structure research to assess subsurface conditions (Arai, H., and Tokimatsu, K., 2004). Key parameters obtained from the HVSR method include the dominant frequency (f0) and seismic wave amplification (A). The dominant frequency indicates the bedrock type, while amplification is influenced by physical rock properties like weathering or deformation, varying with changes in the same rock body.

This study seeks to use geoelectric data processing methods, such as *Electrical Resistivity Tomography* (ERT), and microtremor measurements with the *Horizontal to Vertical Spectral Ratio* (HVSR) method to map soil characteristics in non-typical Cilembu sweet potato lands. The goal is to create resistivity value distribution maps related to soil fertility in the research area. This research aims to serve as a reference for similar studies on soil fertility in agricultural lands.

Theoretical Background

Soil Geology

Pedology is the study of various geological aspects of soil, including soil formation, physical and chemical characteristics (soil morphology), and soil classification (Hardjowigeno, 2003). There are five soil-forming factors: climate, parent material, organisms, topography, and time. Climate influences soil structure through factors like rainfall and temperature, determining the chemical and physical properties of the soil (Mustofa, 2007). The type of parent material determines the resulting soil's physical and chemical properties during soil formation (Mursito & Kawiji, 2002). Topography impacts soil formation by affecting water absorption, groundwater depth, erosion, and water movement (Supadma & Dibia, 2006). Soil organisms influence organic matter accumulation, nutrient cycles, and stable soil structure

(Supriyadi, 2008). Over time, soil evolves due to continuous weathering and erosion processes, resulting in aging and thinning of soil layers (Sholihin, 2017).

Classification of Soil

In Indonesia, most of the soil is volcanic, originating from volcanic eruptions or decomposed volcanic ash (Ritung et al., 2015). Volcanic soil is highly fertile, especially in hilly areas and volcanic ash deposits along riverbanks. There are two main types: regosols, which are coarse-grained alluvial deposits, and andosols, typically characterized by a gray to brownish appearance (Rosmarkam & Yuwono, 2002).
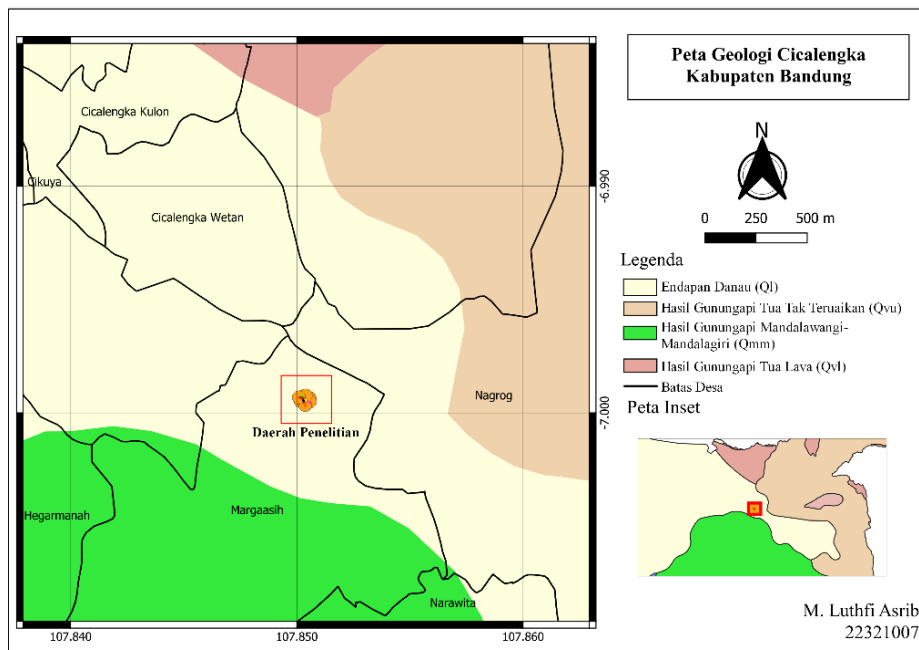
Geology of the Research Area

Figure 2.1 *Geological Map of the Bandung Sheet*

According to the Geological Map of the Bandung Sheet by the Geological Research and Development Center (P. H. Silitonga, 2003), the research area consists of Lake Deposits (Ql) containing tuffaceous clay, tuffaceous sandstone, tuffaceous gravel, and conglomerate. This area contains limestone concretions, plant remnants, freshwater mollusks, and vertebrate animal bones.

Ideal Criteria for Cilembu Sweet Potatoes

Cilembu sweet potatoes are a popular agricultural commodity known for their distinct sweetness and sugary secretion. They come from Cilembu Village in Sumedang Regency, West Java, which has earned a Geographical Indication certificate for these sweet potatoes. The primary cultivation areas for Cilembu sweet potatoes are Pamulihan, Tanjungsari, Rancakalong, and Sukasari. Ideal conditions for sweet potato growth include temperatures of 21-27°C, 11-12 hours of daylight, and annual rainfall between 750-1,500 mm. They thrive in well-drained, loamy sandy soil with good organic content, proper aeration, and pH levels of 5.5-7.5. The optimal elevation range is 500-1,000 meters above sea level,

typically between 30°S and 30°N latitude, as they prefer warm and humid conditions (Arif Kurniawan, 2008).

Design Survey of Research Area

The research is conducted in the land of Margaasih Village, Cicalengka District, Bandung Regency, West Java. The area has a westward sloping topography and experiences a tropical climate influenced by monsoons, with annual rainfall between 1,500 mm and 2,300 mm. Temperature ranges from 20°C to 26°C, with humidity varying from 78% during the rainy season to 70% in the dry season. For ERT (Electrical Resistivity Tomography), there are 6 lines as shown in Figure 1.1, with each line having 48 electrodes spaced 30 cm apart. Consequently, the length of each line is 14 meters. The estimated depth for ERT is up to 2 meters. For HVSR (Horizontal to Vertical Spectral Ratio), there are a total of 12 microtremor measurement points.
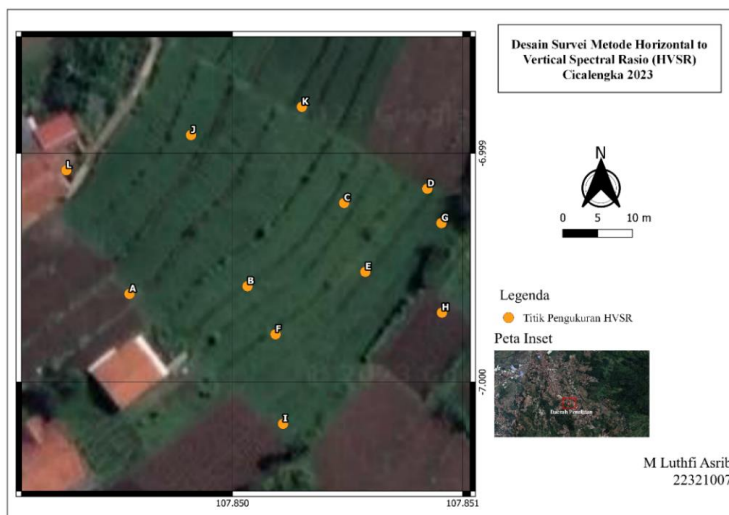

Figure 2.2 Design Survey of HVSR

Figure 2.3 Design Survey of ERT

Method

Electrical Resistivity Tomography (ERT)

Electrical Resistivity Tomography (ERT) is a geophysical method that assesses subsurface resistivity by injecting electrical current into the ground. ERT is used for various applications, including groundwater level determination, geological structure investigations, and mineral exploration (Reynolds, 2011). ERT works by injecting electric current through electrodes and measuring it with potential electrodes. The resulting data, known as apparent resistivity, is processed using inversion techniques and software like RES2DINV to obtain true resistivity values. Apparent resistivity offers a qualitative view of subsurface resistivity distribution in non-homogeneous media (Reynolds, 2011). Apparent resistivity values can be calculated as follows:

$$\rho_a = K\,\frac{V}{I} \qquad\qquad \text{III.1}$$

with ρa representing apparent resistivity, K as the geometric factor, V as electric potential, and I as electric current. The value of K depends on the electrode configuration used in the measurement. In general, K can be expressed as:

$$K = 2\pi \left[\frac{1}{AM} - \frac{1}{MB} - \frac{1}{AN} + \frac{1}{NB}\right]^{-1} \qquad\qquad \text{III.2}$$

Where AM is the distance between A and M, MB is the distance between M and B, AN is the distance between A and N, and NB is the distance between N and B (see Figure 3.1 for a better illustration).
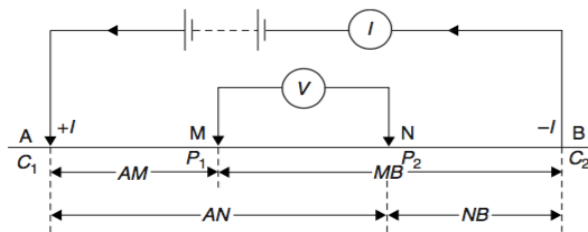

Figure 3.0.1 illustration of the electrode configuration model

In this study, the chosen electrode configuration is the Wenner-Schlumberger configuration. It is preferred for its sensitivity to local inhomogeneities, providing better results for detecting changes in both vertical and horizontal resistivity (Loke and Barker, 1996). The Wenner-Schlumberger array is similar to the Wenner Alpha array, with potential electrodes (A and B) and current electrodes (M and N) spaced "n" times farther apart than the two potential electrodes. The equation for the Wenner-Schlumberger array can be expressed as:

$$\rho_a = 2\pi \left[\frac{1}{AM} - \frac{1}{MB} - \frac{1}{AN} + \frac{1}{NB} \right]^{-1} \left(\frac{V}{I} \right) \qquad \text{III.3}$$

$$\rho_a = \pi n(n + 1)a \left(\frac{V}{I} \right) \qquad \text{III.4}$$

Loke in 1999 created an ERT interpretation guide that covers the typical resistivity and conductivity ranges for hard rocks, soft rocks, and soils. The range descriptions are as follows:

Table 1. Material Resistivity Table

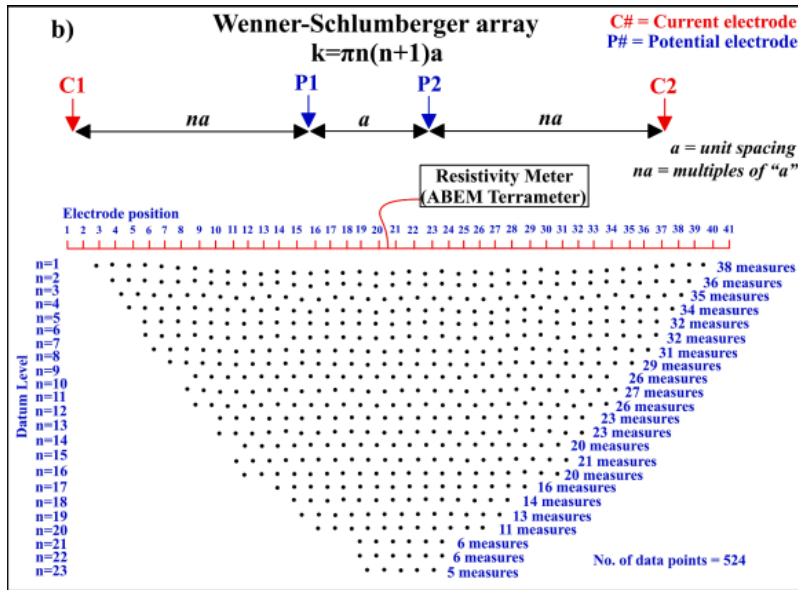| Jenis Material	Resistivitas (Ωm)
Igneous and Metamorphic	
Rocks	
	$5 \times 10^3 - 10^6$
Granite	
	$10^3 - 10^6$
Basalt	
	$6 \times 10^2 - 4 \times 10^7$
Slate	
	$10^2 - 2.5 \times 10^8$
Marble	
	$10^2 - 2 \times 10^8$
Quartzite	
	$10^2 - 10^8$
Sedimentary Rocks	
Sandstone	
	$8 - 4 \times 10^3$
Shale	
	$20 - 2 \times 10^3$
Limestone	
	$50 - 4 \times 10^2$
Soils and Water	
Clay	1-100
Alluvium	10-800
Groundwater	10-100
Sea Water	0.2

Figure 3.2 Wenner-Schlumberger Array (Kumar dkk., 2021)

The data collection process is carried out using the Electrical Resistivity Tomography (ERT) method with the Wenner-Schlumberger configuration. The positions of the current and potential electrodes are arranged as shown in Figure 4.

The geoelectric data is collected by passing an electric current between current electrodes and measuring the potential difference between potential electrodes at a specific distance (Fukue et al., 1999). The research data includes measurements like electrode distances, current, potential difference, geometric factors, and apparent resistivity. During data collection, cross-checking is done to ensure data accuracy and quality control (McCarter, 1984; Michot et al., 2000). Data processing is carried out using RES2DINV software, which generates cross-sections depicting subsurface layers with their true resistivity values. These 2D inversion models help identify soil types based on rock weathering products observed in the ERT cross-sections (Edwards, 1977).

Horizontal to Vertical Spatial Ratio **(HVSR)**

The HVSR (Horizontal to Vertical Spectral Ratio) method was initially introduced by Nogoshi and Igarashi (1971) and later popularized by Nakamura (1989), known as the Nakamura technique. The Nakamura HVSR method is an empirical technique used to estimate the resonance characteristics of subsurface layers. Important parameters derived from the HVSR method include the dominant frequency (f0) and amplification factor (A). These parameters are related to subsurface physical properties (Herak, 2008).

Based on Nakamura's observations in 1989, recordings at stations located on hard rock typically have a maximum ratio of horizontal to vertical component spectra close to one. In contrast, in soft layers, the ratio of horizontal to vertical component spectra has a maximum value greater than one. The magnitude

of the horizontal amplification factor (T_H) is expressed by the following equation III.5:

$$T_H = \frac{SH_S}{SH_R}$$

III.5

SH_S is the spectrum of the horizontal component in the sediment layer, and SH_B is the spectrum of the horizontal component in the bedrock. The vertical amplification factor (T_V) is expressed by the following equation III.6:

$$T_V = \frac{SV_S}{SV_B}$$

(III.6

SV_S is the spectrum of the vertical component in the sediment layer, and SV_B is the spectrum of the vertical component in the bedrock. According to Nakamura (1989), microtremors disregard surface waves and are dominated by shear waves. Therefore, HVSR is considered analogous to the vibration transfer function of seismic waves in sediment layers and bedrock. Hence, the peak frequency and amplitude of HVSR represent local amplification and frequency.

The noise recorded on bedrock due to the effects of Rayleigh waves can be eliminated because the spectrum ratio between the horizontal and vertical components on bedrock approaches one. This means that only the influence of local geological structure (*TSITE*) explains the peak amplification at the fundamental frequency of a location. Therefore, the value of HVSR can be expressed as shown in equation III.7:

$$HVSR = T_{SITE} = \frac{\sqrt{(H_{NS}(f))^2 + (H_{EW}(f))^2}}{SV_S}$$

(III.7

where H_{NS} represents the spectrum of the north-south horizontal component, H_{EW} represents the spectrum of the east-west horizontal component, and SV_S denotes the spectrum of the vertical component.

Result and Discussions

Results

The HVSR curves from each station displayed conform to the criteria for HVSR curves as described in the guidelines by Acerra, C., et al. (2004).
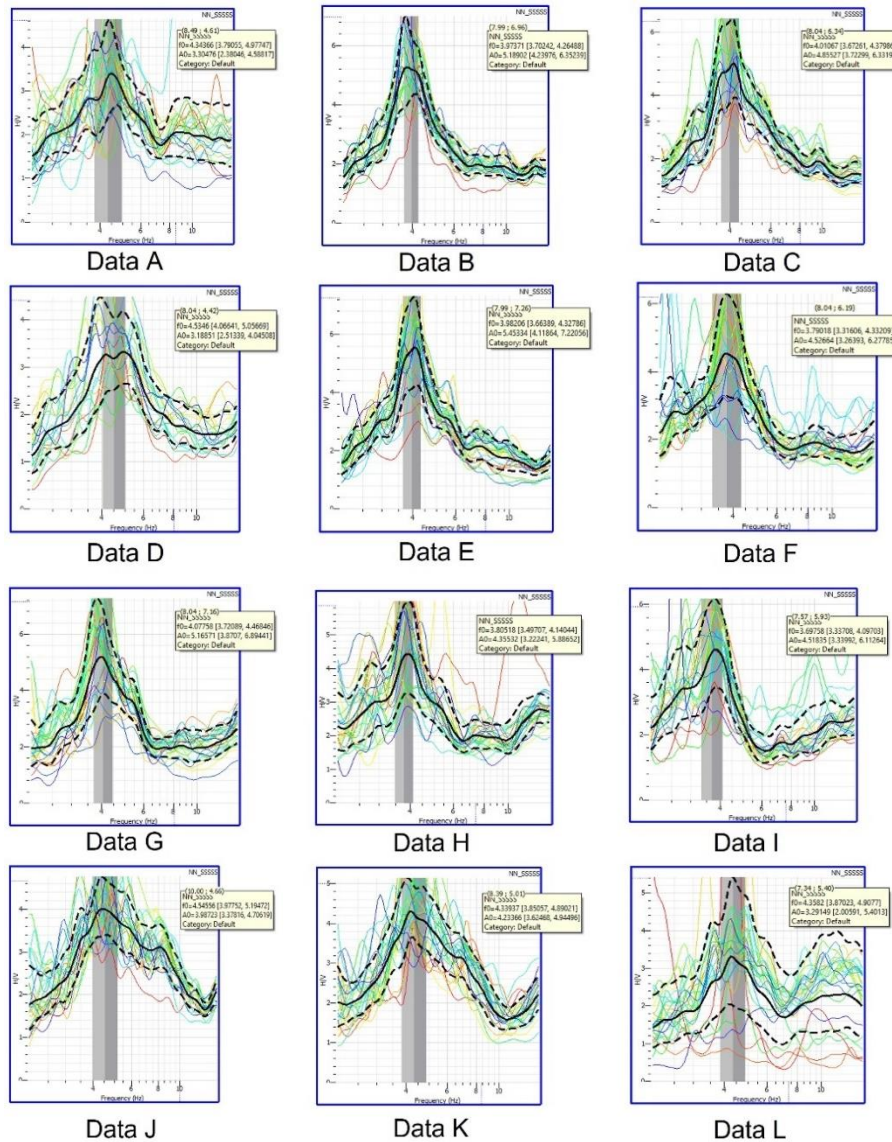

Figure 4.1 *HVSR curve points A to L*

Figures 4.1 display the HVSR curves obtained from the processing of each microtremor measurement point. From the HVSR curves, it can be determined that the volcanic soil in the research area has f0 values ranging from 3.697 to 4.545 Hz and A values ranging from 3.1 to 5.4. According to the soil classification table by Kanai (1989), the research area generally falls under Type III-IV classification, Type II-III, with a classification of alluvial rock with a thickness of 10-30 meters. It consists of sandy-gravel, sandy hard clay, loam, and tertiary or older rock soil composed of hard sandstone and gravel, with a thick surface sediment layer dominated by hard rock.
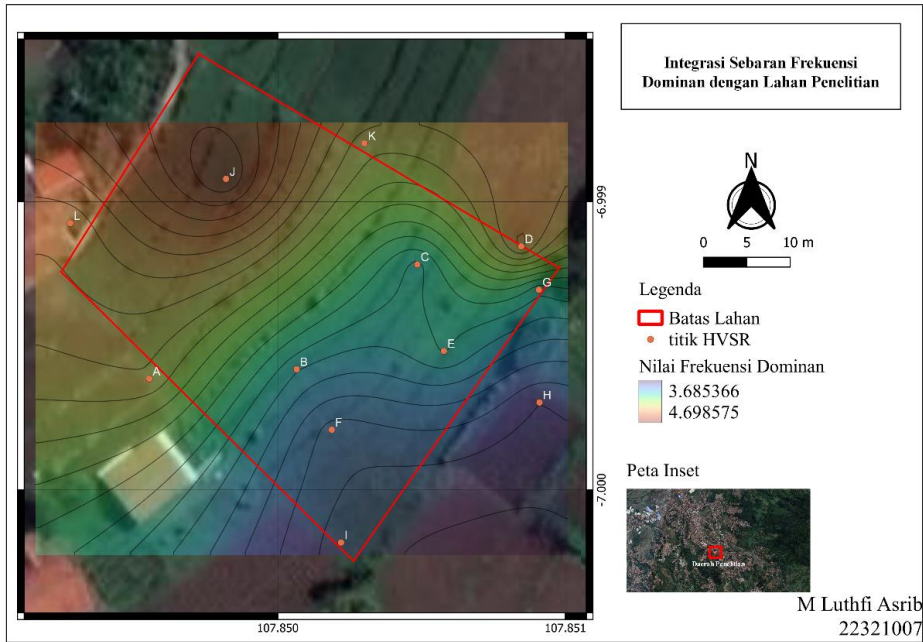
Figure 4.2 dominant frequency distribution

Based on the range of dominant frequency values, the research area is divided into three types: agricultural areas with a moderate dominant frequency of 4 - 4.4 Hz, represented in green, indicating a moderate sediment thickness; areas with a low dominant frequency (f0 < 4 Hz), shown in blue-purple, representing thicker sediment layers; and areas with a high dominant frequency (f0 > 4.5 Hz), shown in yellow-red, indicating relatively thin sediment layers. In the agricultural areas with dominant frequency values below 4, it signifies that these areas have thicker sediments. This is due to the topography of the land sloping from east to west, resulting in elevation differences in agricultural fields. These elevation differences lead to variations in sediment thickness. The thickness of the sediment affects the distance between plant roots and groundwater. The thicker the sediment, the farther the plant roots need to reach for water, making it challenging for plants to grow.
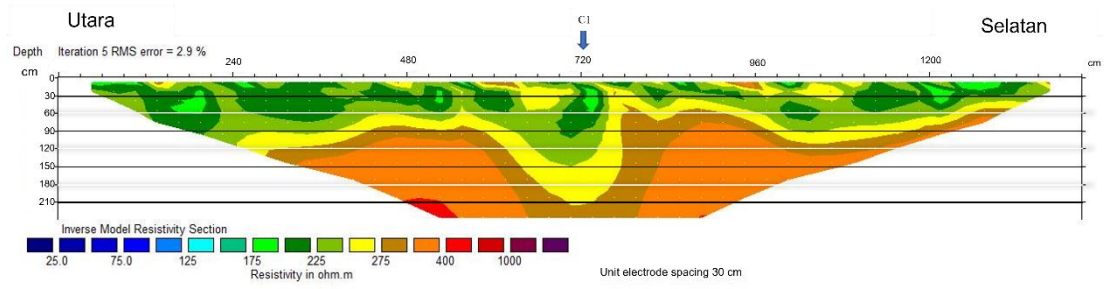
Figure 4.3 distribution of amplification factors

Based on the map of amplification distribution, the color blue represents low amplification (<4), green and yellow represent moderate amplification (4 - 4.5), and orange represents high amplification (>4.5). In agricultural areas with amplification values above 4, it indicates that the soil is heterogeneous and relatively dense, allowing it to absorb water better. Consequently, the soil in these areas is more fertile compared to areas with low amplification (<4), which may signify denser or harder soil. Amplification values represent the contrast in soil density and can indicate the level of soil homogeneity in agriculture. Low amplification values indicate that there are no significant differences in physical properties between layers (homogeneous), and soil homogeneity is a result of the same weathering processes.

The results of Electrical Resistivity Tomography (ERT) data processing consist of 2D cross sectional images based on each surveyed profile. Here are the interpretation results for each survey profile.

Figure 4.4 Cross-sectional results of Track 1

Figure 4.5 Cross-sectional results of Track 2
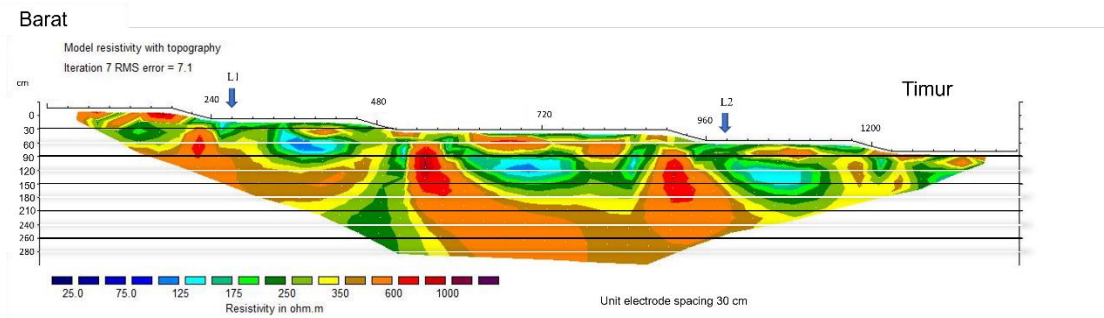

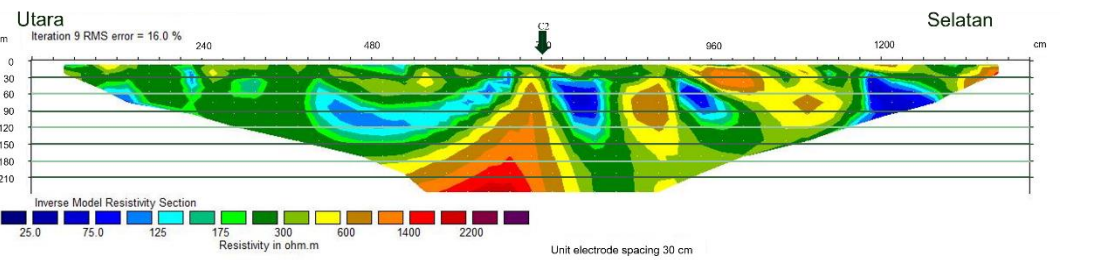*Figure 4.6 Cross-sectional results of Track 6*

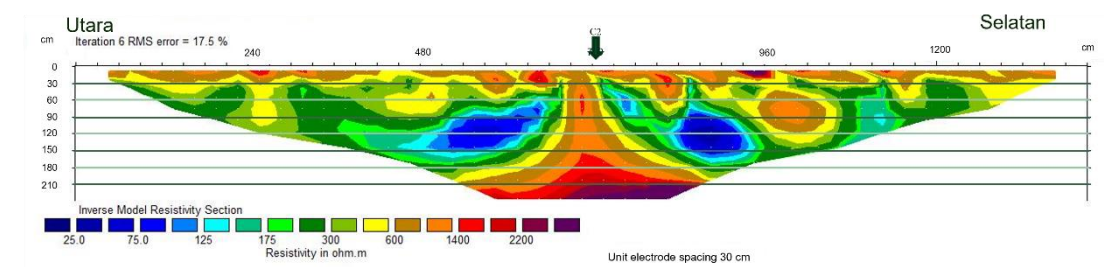*Figure 4.7 Cross-sectional results of Track 3*

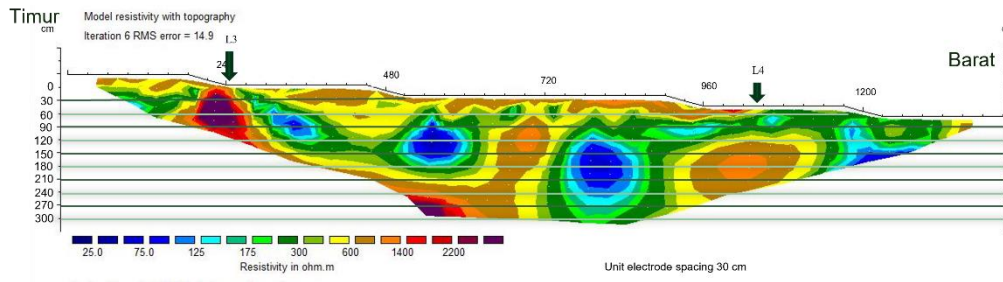*Figure 4.8 Cross-sectional results of Track 4*

Figure 4.9 Cross-sectional results of Track 5

In Figure 4.4, the first layer is depicted in shades of light green to dark green, with a depth of 0-90 cm and resistivity values ranging from 175-225 Ωm. This layer is indicated as the O horizon, consisting of organic material with a low mineral fraction. The second layer, colored in shades of yellow to brownish-yellow, extends from a depth of 90-150 cm and has resistivity values ranging from 250-300 Ωm. This layer is identified as the A horizon (Subsurface), resulting from the accumulation of fine organic material that has decomposed and mixed with minerals from the parent rock in the soil. The bottommost layer is depicted in orange, with a depth greater than 150 cm and resistivity values up to 400 Ωm. This layer is identified as the B horizon (Subsoil), and it has undergone significant to complete horizon development, characterized by the disappearance of most to all original rock structures.

In Figure 4.5, the first layer is shown in shades of light green to dark green, with a depth of 0-60 cm and resistivity values ranging from 175-225 Ωm. Similar to profile 1, this layer is indicated as the O horizon, composed of organic material with a low mineral fraction. The second layer, colored in shades of yellow to brownish-yellow, extends from a depth of 60-150 cm and has resistivity values ranging from 250-300 Ωm. This layer is also identified as the A horizon (Subsurface), resulting from the accumulation of fine decomposed organic material mixed with minerals from the parent rock in the soil. The bottommost layer is depicted in orange, with a depth greater than 150 cm and resistivity values exceeding 400 Ωm. This layer is also identified as the B horizon (Subsoil), and it has undergone horizon development, with most to all of the original rock structures being eroded, similar to profile 1. In this profile, there is a noticeable phenomenon of the O horizon lowering from electrode 18 to electrode 25 over a length of 2.1 meters. This is believed to be the result of surface soil activity or the accumulation of water and minerals in that area.

The profile shown in Figure 4.6 is the result of a crossing between traverse 1 and traverse 2. This was done to observe the distribution of resistivity values with a different orientation (East-West). In Figure IV.7, the first layer is indicated by light blue to dark green with a depth of 30-90 cm and resistivity values ranging from 75-350 Ωm. This layer is interpreted as an aquifer or a soft zone. The second layer, indicated by yellow to brownish-yellow colors, has a depth of 90-210 cm and resistivity values ranging from 350-600 Ωm, suggesting a dry zone. The bottommost layer, depicted in orange, extends beyond 60-300 cm in depth and has resistivity values exceeding 600 Ωm, indicating bedrock or the parent rock material. The cross-sectional view shows the westward movement of the soil, likely due to the decreasing elevation from east to west.

In Figure 4.7, the first layer is depicted with light blue to dark green colors at a depth of 30-150 cm, having resistivity values ranging from 75-300 Ωm. This layer is interpreted as an aquifer or a soft zone. The second layer, indicated by yellow to brownish-yellow colors, is found at the surface with a depth of 0-30 cm and reappears at 60-150 cm in depth, with resistivity values ranging from 600-1400 Ωm,

suggesting a dry zone. The bottommost layer, shown in orange, extends beyond 180 cm in depth and has resistivity values exceeding 2000 Ωm, indicating bedrock or the parent rock material. The higher resistivity values near the surface are attributed to the dry conditions during data acquisition, which results in higher resistivity values when electric current is injected into the dry soil.

In Figure 4.8, the first layer is depicted with light blue to dark green colors, extending to a depth of 0-150 cm and having resistivity values ranging from 75-300 Ωm. This layer is interpreted as an aquifer or a soft zone. The second layer, indicated by yellow to brownish-yellow colors, is found at a depth of 90-150 cm with resistivity values ranging from 600-1400 Ωm, suggesting a dry zone. The bottommost layer, shown in orange, extends beyond 180 cm in depth and has resistivity values exceeding 2000 Ωm, indicating bedrock or the parent rock material.

The results shown in Figure 4.9 represent a cross-section that intersects Tracks 3 and 4, with an RMS error value of 14.9%. This was done to observe the distribution of resistivity values with an orientation perpendicular to Tracks 3 and 4 (East-West). From this cross-section, it can be interpreted that the layers formed still exhibit varying resistivity values. The colors range from dark blue to dark green (75-300 Ωm), indicating an aquifer or a soft zone. The yellow to brownish-yellow colors (600-1400 Ωm) are interpreted as a dry zone, while the red to purple colors (>2000 Ωm) indicate hard rock or bedrock.

Discussions

The integration of dominant frequency with the 2D Electrical Resistivity Tomography (ERT) cross-section is essential to provide complementary information about sediment thickness. This integration can be observed in Figure 4.10 In the image, the upper land has low-frequency values, indicating thick sediment dominated by soil with low resistivity values ranging from 175-400 Ωm. This suggests that the upper land has experienced significant weathering, resulting in sediment thickening in that area. In contrast, the lower land exhibits high-frequency values, indicating thin sediment with soil dominated by moderate resistivity values ranging from 300-1000 Ωm. This implies that the lower area is still undergoing development or weathering, with the bedrock still being the dominant feature.
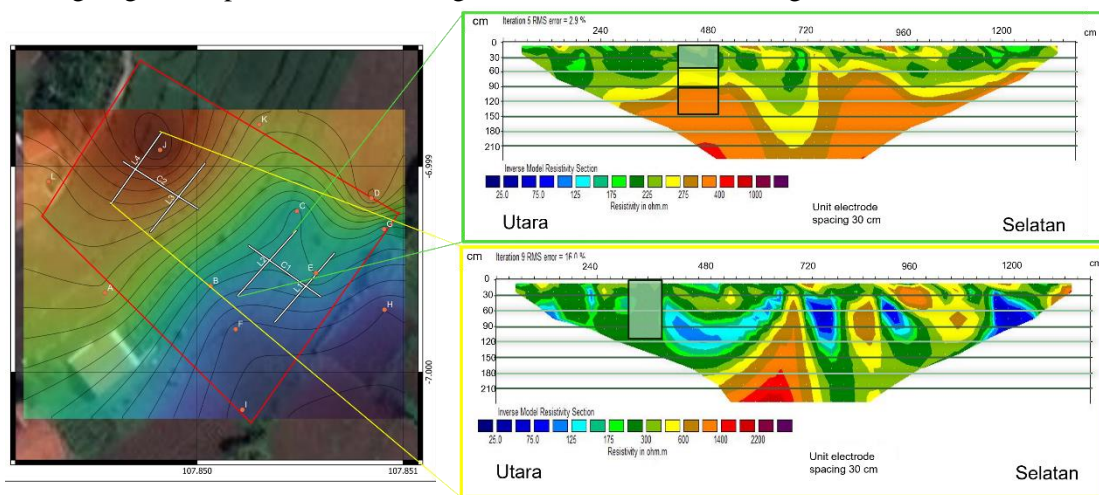

Figure 4.10 Dominant frequency integration with Electrical Resistivity Tomography (ERT)

The integration of amplification with the 2D Electrical Resistivity Tomography (ERT) cross-section is necessary to provide complementary information about soil homogeneity. This integration can be observed in Figure IV.16. In the image, the upper land exhibits high amplification values, indicating

low soil homogeneity or soil heterogeneity in that area due to ongoing weathering. The contact between organic and mineral materials can create differences in physical characteristics, especially soil density. This corresponds to the cross-section image of track 2, which depicts well-defined layers, suggesting that weathering has occurred evenly.In contrast, the lower land has low amplification values, indicating a high level of soil homogeneity. This suggests that the soil in this area has a high level of density. This aligns with the cross-section image of track 4, which shows abstract layering due to ongoing weathering and a dominance of bedrock properties.
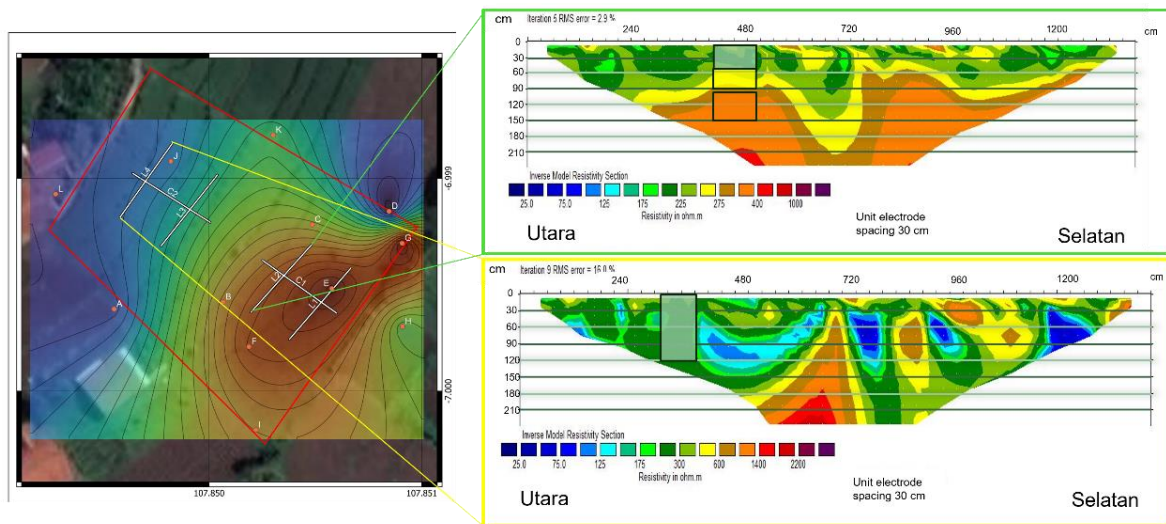

Figure 4.11 Amplification integration with Electrical Resistivity Tomography (ERT)

From the perspective of soil types in the non-typical area, the soil tends to be clayey and muddy, as indicated by soil resistivity values ranging from 25-800 Ωm and sieve tests showing an average percentage in the samples. This means that this type of soil acts as a hindrance to root growth in terms of both spread and size. The clayey texture of the soil makes it difficult for roots to penetrate and expand. As a result, sweet potatoes are likely to be smaller and elongated in this type of soil.

Conclusions

Based on the research results presented above, several conclusions can be drawn:
1. The non-typical area of Cilembu sweet potatoes has a dominant frequency range from 3.697 to 4.545 Hz and amplification values ranging from 3.1 to 5.4. With these values, there is a variation in sediment thickness and soil homogeneity levels from east to west
2. The resistivity values in the non-typical Cilembu sweet potato fields vary significantly at different depths, ranging from 25 to 2000 Ωm. With this range, the soil can be classified as alluvial soil, ranging from silt to clay.
3. From the correlation between the interpretation of amplification and dominant frequency values, the 2D Resistivity cross-section, trench test results, mineral and sieve analysis, the characterization of the land reveals a thick horizon O with limited macro-nutrients support for plant growth, and suboptimal root development due to the clayey soil texture, which makes it difficult for the roots to penetrate and expand. As a result, sweet potatoes are likely to be smaller and elongated in this type of soil.

These conclusions provide valuable insights into the specific conditions of the non-typical Cilembu sweet potato cultivation area, helping to understand the variations in soil properties, sediment thickness, and the challenges posed for crop growth.

References

Aizebeokhai, A. P. (2014). Assessment of soil salinity using electrical resistivity imaging and induced polarization methods. *African Journal of Agricultural Research, 9*(45), 3369-3378.

Arai, H., & Tokimatsu, K. (2004). S-wave velocity profiling by inversion of microtremor H/V spectrum. *Bulletin of the Seismological Society of America*, 94(1), 53-63.

Arifin, M. Z., Anwar, K., & Simatupang, R. S. (2006). Karakteristik dan potensi lahan rawa lebak untuk pengembangan pertanian di Kalimantan Selatan. *Dalam*, 85-102.

Barry, M. A dan Susylowati (2004). Pengaruh Pemupukan N, P, K dan Kepadatan Tanaman Jagung Semi Dalam Sistem Tumpangsari Terhadap Pertumbuhan dan Hasil Jagung Semi (Zea mays L.) dan Kacang Panjang (Vigna sinensis L.). *Jurnal Budidaya Pertanian*. 10(2): 129-138.

Dafalla, M. A., & AlFouzan, F. A. (2012). Influence of physical parameters and soil chemical composition on electrical resistivity: a guide for geotechnical soil profiles. *Int J* Electrochem Sci, 7, 3191-3204.

Edwards, L. S. (1977). A modified pseudosection for resistivity and IP. *Geophysics*, 42(5), 1020-1036.

Fukue, M., Minato, T., Horibe, H., & Taya, N. (1999). The micro-structures of clay given by resistivity measurements. *Engineering geology*, 54(1-2), 43-53.

Ganiyu, S. A., Olurin, O. T., Oladunjoye, M. A., & Badmus, B. S. (2020). Investigation of soil moisture content over a cultivated farmland in Abeokuta Nigeria using electrical resistivity methods and soil analysis. *Journal of King Saud University-Science, 32*(1), 811-821.

Hanafiah, K. A. (2007). Dasar-Dasar Ilmu Tanah Jakarta: *PT. Raja Grafindo Persada.*

Hardjowigeno, S. (2003). *Ilmu Tanah*. Jakarta, Indonesia: Akademika Pressindo.

Herak, M. (2008). Model HVSR—A Matlab® tool to model horizontal-to-vertical spectral ratio of ambient noise. Computers & Geosciences, 34(11), 1514-1526.

Kearey, P., Brooks, M., Hill, I., 2002. An introduction to geophysical exploration. Blackwell Science.

Kumar, P., Tiwari, P., Singh, A., Biswas, A., & Acharya, T. (2021). Electrical Resistivity and Induced Polarization signatures to delineate the near-surface aquifers contaminated with seawater invasion in Digha, West-Bengal, India. *Catena, 207*, 105596.

Lowrie, W., & Fichtner, A. (2020). *Fundamentals of geophysics*. New York, United Kingdom: Cambridge University Press.

Loke, M. H. (1999). A Practical Guide to 2D and 3D Surveys. *Electrical Imaging Surveys for Environmental and Engineering Studies*, 8-10.

Lumenta, E., & Setiawan, T. (2019). Metode Pemetaan Resistivitas Tanah pada Survei Pertanian dengan HUMA EC 1. *Jurnal Geofisika, 15*(2), 21-25.

McCarter, W. J. (1984). The electrical resistivity characteristics of compacted clays. *Geotechnique*, 34(2), 263-267.

Michot, D., Benderitter, Y., Dorigny, A., Nicoullaud, B., King, D., & Tabbagh, A. (2003). Spatial and temporal monitoring of soil water content with an irrigated corn crop cover using surface electrical resistivity tomography. *Water Resources Research*, 39(5).

Mursito, D. dan Kawiji (2002). Pengaruh Kerapatan Tanam dan Kedalaman Olah Tanah Terhadap Hasil Umbi Lobak (Raphanus sativus L.). *Agrosains*. 4(1): 1-6

Mustofa, A. (2007). Perubahan Sifat Fisik, Kimia, dan Biologi tanah pada Hutan Alam yang diubah Menjadi Lahan Pertanian di Kawasan Taman Nasional Gunung Leuser. Jurusan Silvikultur. Fakultas Kehutanan. IPB. Bogor. Skripsi.

Reynolds, J. M. (2011). *An introduction to applied and environmental geophysics*. Chichester, United Kingdom: John Wiley & Sons.

Ritung, S., Suryani, E., Subardja, D., Nugroho, K., Mulyani, A., Tafakresnanto, C., ... & Supriatna, W. (2015). Sumber daya lahan pertanian Indonesia: luas, penyebaran, dan potensi ketersediaan. IAARD Press.

Rosmarkam, A., & Yuwono, N. W. (2002). Ilmu Kesuburan Tanah Yogyakarta (ID): Kanisius.

Silitonga, P.H. (2003). *Geologi Lembar Bandung, Skala 1:100.000*, Pusat Penelitian dan Pengembangan Geologi. Departemen Pertambangan dan Energi.

Solihin, M. A., Sitorus, S. R. P., Sutandi, A., & Widiatmaka, W. (2016). Karakteristik Lahan dan Kualitas Kemanisan Ubi Jalar Cilembu. *Journal of Natural Resources and Environmental Management* , 7(3), 251-259.

Solihin, M.A. 2017. Model Penentuan Kriteria Kesesuaian Lahan Ubi Jalar Cilembu Varietas Rancing Berbasis Karakteristik Spesifik Lokasi. Disertasi. Institut Pertanian Bogor. Bogor

Sudha, K., Israil, M., Mittal, S., & Rai, J. (2009). Soil characterization using electrical resistivity tomography and geotechnical investigations. *Journal of Applied Geophysics*, *67*(1), 74-79.

Supadma, A.A., I.N. Dibia. (2006). Evaluasi Status Kesuburan Tanah Sawah di Kelurahan Penatih Kota Denpasar Untuk Perencanaan Pemupukan Berimbang. *Jurnal Agritrop* 25(4):116-124.

Supriyadi, S. (2008). Kandungan Bahan Organik Sebagai Dasar Pengelolaan Tanah di Lahan Kering Madura. *Jurnal Embryo* 5(.2):180

Susanto, E., Herlina, N., & Suminarti, N. E. (2014). Respon pertumbuhan dan hasil tanaman ubi jalar (Ipomoea batatas L.) pada beberapa macam dan waktu aplikasi bahan organik. *Jurnal produksi tanaman*, 2(5), 412-418.

Wandana, S., Hanum, C., & Sipayung, R. (2012). Pertumbuhan dan hasil ubi jalar dengan pemberian pupuk kalium dan triakontanol. *Jurnal Online Agroekoteknologi*, 1(1) : 199-211.

Widijanto, H., Syamsiyah, J., & Ferela, B. D. I. (2008). Efisiensi serapan p tanaman kentang pada tanah andisol dengan penambahan vermikompos. *Sains Tanah-Journal of Soil Science and Agroclimatology*, 5(2), 67-74.